Bringing Monsoonal Conditions West: Connecting African Easterly Waves with Indian Monsoonal Outflow and Divergent Kelvin Waves

Jon Starfeldt[1], Gregory Tripoli[1]

[1] *Department of Atmospheric and Oceanic Sciences, University of Wisconsin-Madison, Madison, WI.*

1. Abstract

A priorly proposed idea that difluence in the Tropical Easterly Jet (TEJ) may be a precursor of particularly intense African Easterly Waves (AEWs) is furthered by investigating the cause for the environmental conditions that help promote this difluence. Conserved low potential vorticity (PV) air is created at the outflow levels of convective storms as a consequence of the upward transport of near-surface environmental lows or negative equivalent potential vorticity by the overturning vertical circulation. Environmental static stability at the outflow level, causes the transported potential vorticity to reduce local static stability at the outflow level and also to reduce the absolute vorticity so as to conserve the transported low equivalent potential vorticity, now dry potential vorticity. The lowered potential vorticity at the outflow level naturally reduced inertial environmental resistance to outflow of further deep convection. Observational based analysis of the low PV outflow from the Indian Monsoon shows it can be transported by the TEJ to Northern Africa, where AEWs form. Baroclinic conditions that tend to form AEWs during the summer months, do not naturally support the deepening of AEW circulations to grow into the Upper Troposphere- Lower Stratosphere (UTLS). The westward movement of conserved low PV air into West Africa during the South Asian Monsoon (SAM) creates the conditions over West Africa for deepening the AEWs into the UTLS.

Further observation of velocity potential (χ) fields, calculated from the 6 hourly ERA-I reanalysis, shows upper-level divergence fields "propagating" eastward, against the flow of the TEJ, in the UTLS, via equatorial Kelvin waves. In this paper, we test the hypothesis that low PV air from the SAM provides environmental conditions beneficial for the upper tropospheric difluence observed to relate to the deepening of AEWs into intense hurricanes and that equatorial Kelvin waves bring divergence fields to further their deep convection. A series of Hovmöller diagrams is used in our analysis, where our hypothesis is well supported. ERA-Interim data is used over the 2017 hurricane season due to its number of particularly strong storms, including Hurricanes Harvey, Irma, and Maria.

2. Introduction

During the Northern hemisphere summer, synoptic-scale disturbances called African Easterly Waves are the main synoptic-scale disturbances in Northern Africa during the summer months. These waves typically have a period of 3-5 days, wavelengths of 2000-4000 km, and speeds of 7-9 m s^{-1} (Burpee 1972; Carlson 1969; Reed and Recker 1971; Reed et al. 1977). They are thought to originate in the mountainous regions of Eastern Africa, near Sudan and Ethiopia (Carlson 1969; Albignat and Reed 1980; Berry and Thorncroft 2005) and are usually preceded by several mesoscale convective systems (Berry and Thorncroft 2005). AEWs start off with an eastward tilt with height but rotate to have a westward tilt as they get closer to the West African coast (Reed and Recker 1971; Pytharoulis and Thorncroft 1999). In the lower troposphere, they are driven by baroclinic instability resulting from the low-level meridional thermal gradient across North Africa. These waves are also known to be a primary cause for Atlantic hurricane activity (Burpee 1972; Landsea et al. 1998; Thorncroft and Hodges 2001).

At the beginning of the northern hemisphere summer, in June and July, these disturbances are shallow baroclinic waves below 500 hPa that are fueled primarily by the aforementioned low-level baroclinic instability. The typical amplitude of these waves is near 700 hPa, at the African Easterly Jet (AEJ) core (Albignat and Reed 1980; Pytharoulis and Thorncroft 1999). South of the AEJ, horizontal and vertical shear of the mean wind are important sources for the energy of the waves (Burpee 1972). AEW growth benefits greatly from the baroclinically unstable state over North Africa laid out by Berry and Thorncroft (2005). The disturbances typically reach their greatest intensity near the West African coast, where there is an abundance of moist, convectively unstable air (Carlson 1998).

For the months of August and September, these disturbances change character from shallow baroclinic waves to deep convective disturbances reaching the tropopause (Duvel 1990; Diedhiou et al. 1999). In these waves, there is a region of strong divergence at 175 hPa, above the trough axis (Reed and Recker 1971). At this point, the disturbance can draw new energy from deep convective processes and associated deep overturning of high theta-e air between the surface and outflow levels.

An important part of this picture is the distribution of potential vorticity during tropical cyclogenesis. Latent heat release during cyclogenesis creates PV at low levels and destroys it at upper levels, concurrently extending the spatial extent of the surface maximum and shrinking the upper-level minimum (Schubert and Alworth 1987). The stratification of the upper, negative PV anomaly and lower, positive PV anomaly is well described by the location of maximum latent heat release (Delden 2003). It is also known that the axis of Rossby waves separates locations of positive and negative rainfall anomalies (Nakamura and Takayabu 2022). We will draw upon these observations to identify processes that are beneficial for the deepening of AEWs.

Krishnamurti et al. (2018) found there to have been a maximum in horizontal difluence of the TEJ at 200 hPa near the West African coast before many of the recent category four and five Atlantic Hurricanes. Krishnamurti's work suggests that the strength of the diffluent pattern may be connected to the strength of the Tibetan high, but this idea is not pursued in depth. We observe that low PV air near the tropopause, created from convection driven by the Indian Monsoon, is transported by the TEJ to West Africa, bringing monsoonal conditions with it. We also observe divergence fields are brought in from the west by equatorial Kelvin waves, which provide favorable conditions for further deep convection of AEWs in the Atlantic Ocean.

We hypothesize that it is this low PV air in the outflow layers of the UTLS that provides environmental conditions beneficial for the upper tropospheric difluence that Krishnamurti observed to relate to the deepening of AEWs into intense hurricanes and that equatorial Kelvin waves bring divergence fields from the west that further this deep convective effect. In this paper, we will test this hypothesis by observing the movement of upper air PV anomalies transported by the TEJ and upper divergence anomalies, primarily through Hovmöller diagrams, and look for a correspondent connection in the sea-level pressure (SLP) field.

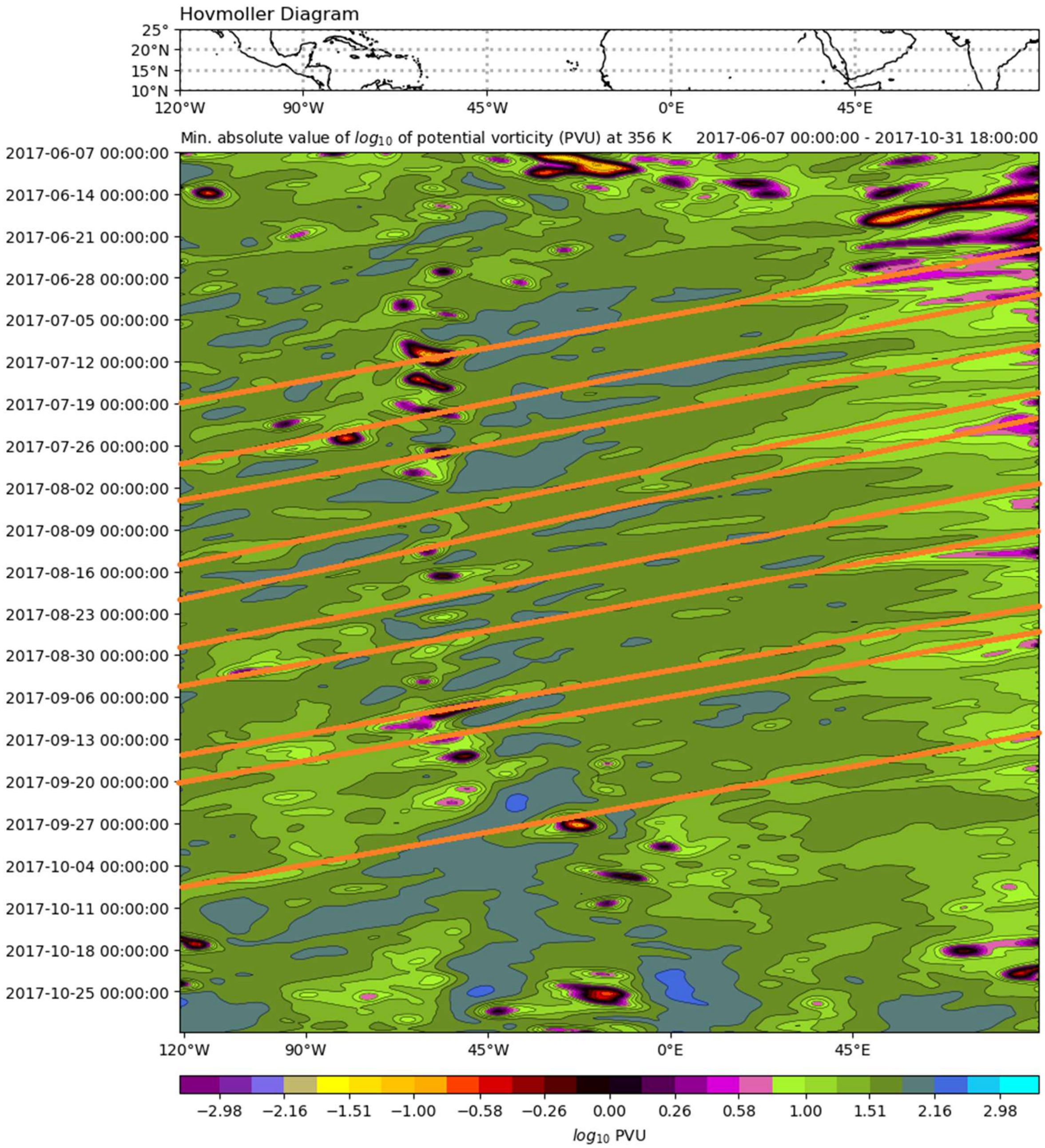

Figure 1: Hovmöller diagram of the $\log_{10}$ of potential vorticity. Colored values show the minimum potential vorticity value across all the latitudes in the defined range at a given time. Orange lines show the approximate propagation of potential vorticity anomalies carried by the Tropical Easterly Jet.

3. Background

In a currently unpublished study by Tripoli on mass injection by tropical cyclone (TC) outflow, PV is examined during the moist adiabatic expansion of the convective overturning process. Ertel PV is defined as

$$PV = -g(\zeta + f)\frac{\delta\theta}{\delta p} \; (1)$$

where ζ is the relative vorticity, f is the Coriolis parameter, and $-\frac{\delta\theta}{\delta p}$ is the static stability. Because the UTLS is characterized by air that is stably stratified and too cold to hold a significant amount of water, PV in the outflow region of deep convective storms can be considered conserved over transport processes. Diabatic changes in PV due to radiative transfer in the outflow area are very small since this elevation lies near the level of zero net radiation. Within *moist* adiabatic processes, such as convective lifting, PV is not fully conserved and can be affected by diabatic processes in the troposphere. Viewing equivalent potential vorticity, using theta-e in place of potential temperature, reveals there is approximate conservation of equivalent potential vorticity across the overturning process. Convective overturning tends to create outflow featuring near-zero or negative dry PV, resulting in an influx of low PV near the tropopause in the tropics. One the lifted air reaches the UTLS, it can flow isentropically outward into its environment creating a low PV plume originating from the core of the overturning circulation.

In Tripoli's study, a cross section of moist PV through Hurricane Patricia reveals a band of low PV along a moist entropy current that is marked by the outflow channels. Examination of vertical stability in the outflow level revealed, in both observations and the model used, a large, positive Brunt-Vaisala frequency, indicating layer stability to be constant. This suggests that changes in the absolute vorticity account for the changes in PV. With the addition of additional low PV air near the outflow level for AEWs, the environmental resistance against outflow by inertial instability should decrease as a consequence. This will allow further mass to be ingested into the UTLS by tropical deep convection, intensifying the AEW.

Equatorial Kelvin waves are tropical weather systems that propagate east along the equator (Takayubu 1994) that typically originate in the Eastern Pacific and Western Atlantic (Mekonnen et al. 2008). Most years have five-six Kelvin waves during the active season, but the most active years can have up to nine (Mekonnen et al. 2008). Local rainfall rates associated with Kelvin wave convection can increase ten-twenty mm compared to the prior day (Mekonnen et al. 2008). In the upper troposphere, near 200 hPa, meridional winds show a divergent pattern associated with convection below. This divergence can be considered a local Hadley circulation response to convective Kelvin wave ascending motion within the precipitation anomalies (Matthews 2021). Looking for divergence fields aloft in the tropics will help us identify where equatorial Kelvin waves may be amplifying convection. Overlapping the divergence fields with AEW propagation can help us understand whether Kelvin waves influence AEW intensity.

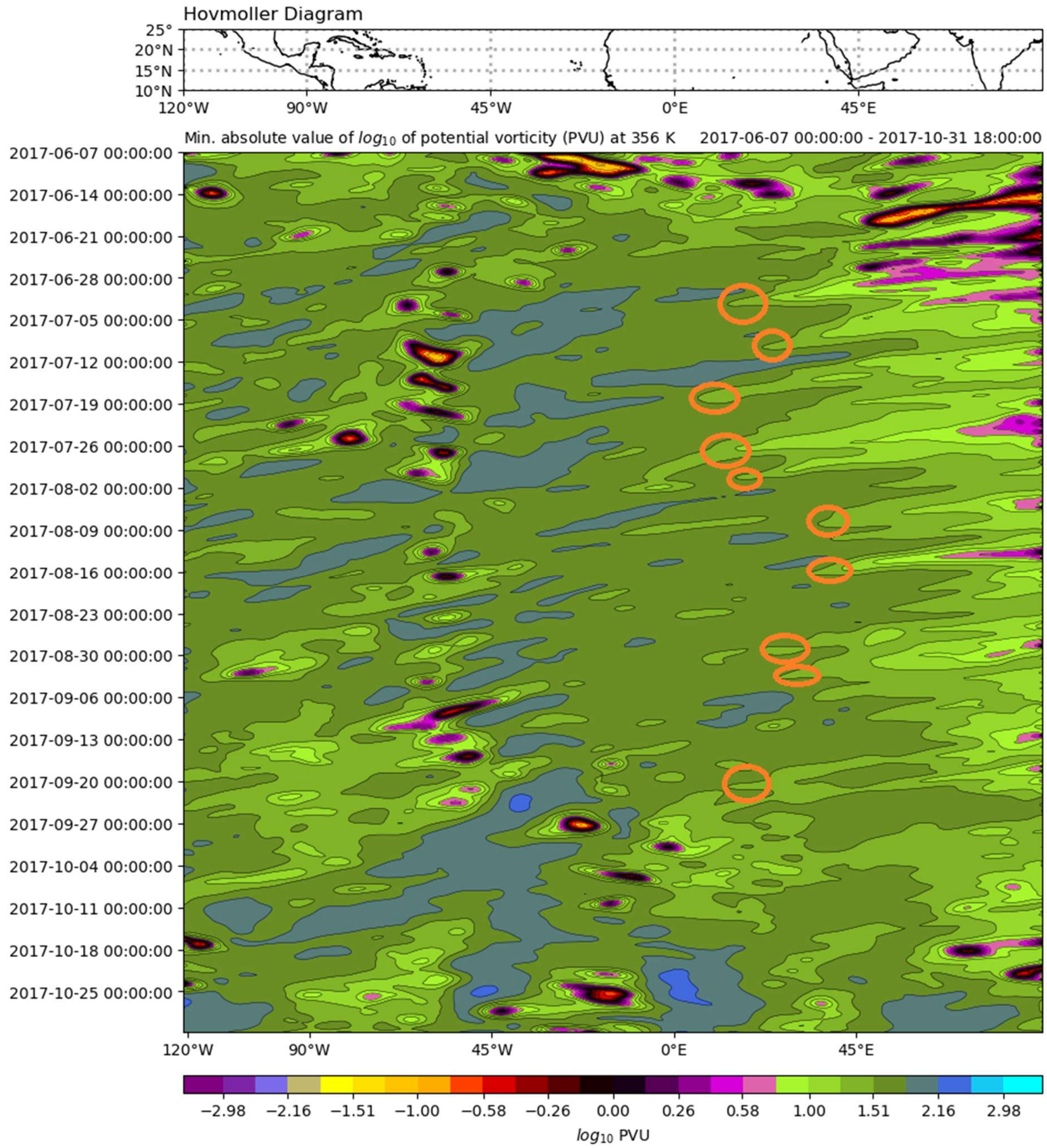

Figure 2: Same diagram as Figure 1, but orange circles depict the ends of potential vorticity plumes flowing from the Indian Monsoon. Identically positioned circles are drawn in Figure 3.

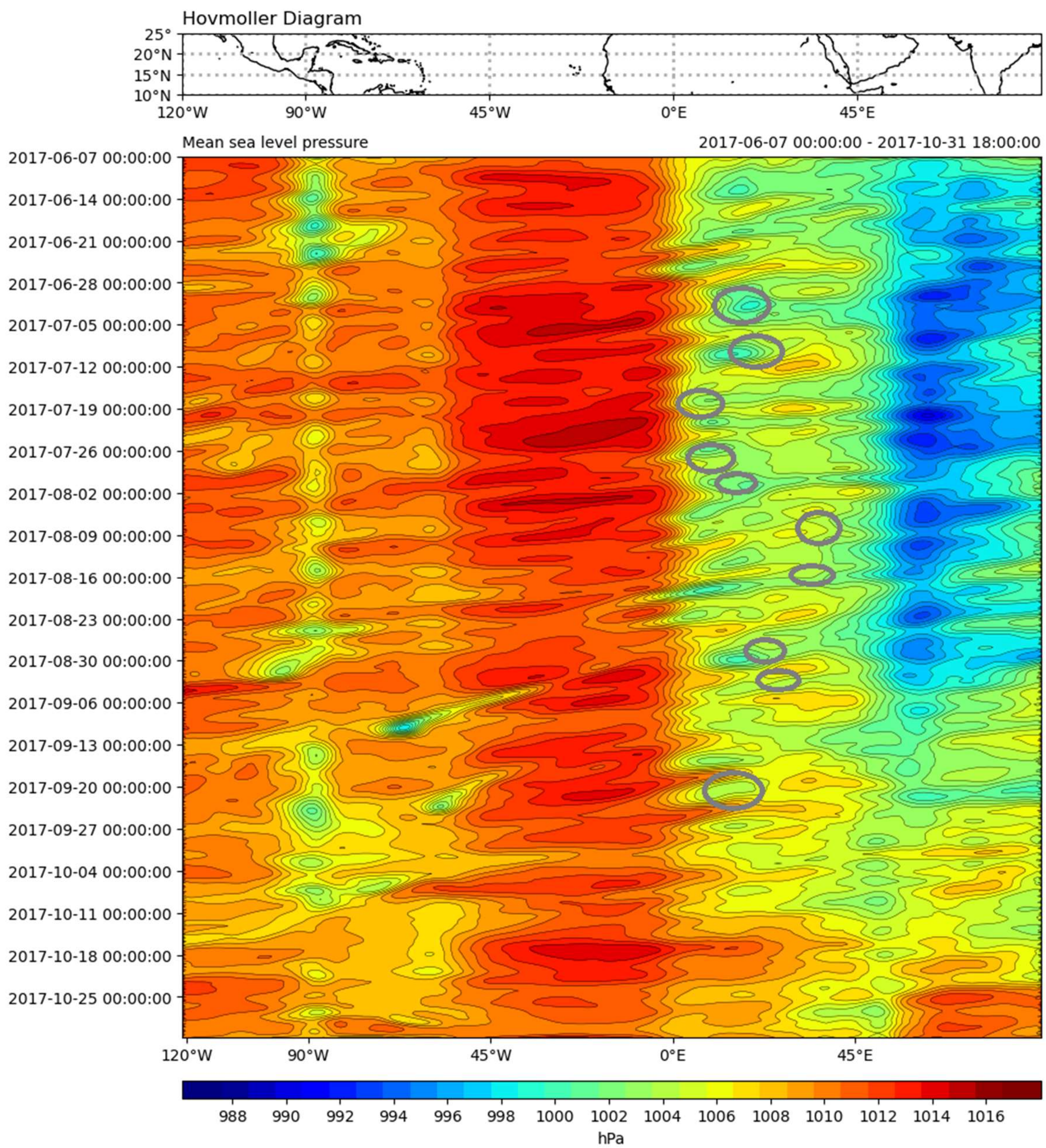

Figure 3: Hovmöller diagram of mean sea level pressure. Colored values show the minimum pressure value across all the latitudes in the defined range at a given time. Circles are identically positioned to the circles in Figure 2 and are used to identify pressure minimums associated with deepening African Easterly Waves.

4. Methods

We show the movement of anomalies using Hovmöller diagrams. Hovmöller diagrams show values over a time-space plane, with values in a single column of longitude or row of latitude aggregated, normally by taking the average, onto one axis. This leaves either latitude or longitude on one axis and time on the other axis. Hovmöller diagrams excel at showing movement in static pictures, hence our use of them in this study. You can learn more about Hovmoller diagrams in Persson (2017).

We defined our area of interest between 10N and 25N latitude and 120W and 90E longitude, which covers the full length of the Atlantic Ocean and slightly into the Pacific Ocean to the west, India to the east, and the Sahara north to south. In our Hovmöller diagrams, time is on the y-axis between June 7 and October 31, 2017, and we aggregate across latitudes so that longitude is on the x-axis.

Our variables of interest were PV (to show swaths of PV flowing from the Indian Monsoon), velocity potential (χ, where negative χ shows divergence and positive χ shows convergence, to investigate divergence fields), and sea-level pressure (to show corresponding deepening of waves at the surface). In each of our Hovmöller diagrams, we aggregate these values as their minimum values across the defined latitude range because we were primarily interested in looking at near-zero PV values that would support instability at upper levels, strong divergence fields ($-\chi$) at upper levels, and low SLP values at the surface.

As described in Section 3, the dry, stable conditions near the UTLS allow for transport of anomalies at upper levels to be an adiabatic process. Because of this, we examine PV and χ on constant potential temperature surfaces. Calculating the potential temperature surface to be used was a multi-step process. First was calculating the propagation speed of the disturbances associated with the AEWs. This was done by drawing lines showing the propagation of PV swaths across its Hovmöller diagram, then taking the distance traveled from east to west across our region of interest and dividing by the time difference between the top and the bottom of the lines. The lines used to calculate the speed are in Figure 1. This speed was averaged across multiple lines and then the height in the dataset that had an average wind speed in our region of interest closet to that average speed was taken. Then, the average potential temperature of the data at the taken height, in our region of interest, was determined to be the appropriate potential temperature to observe these anomalies at. This value was 356 K, which non-coincidently is the approximate level of zero net radiation.

To test the hypothesis that PV anomalies from the Indian Monsoon create an environment favorable for the deepening of AEWs, we followed anomalies of low PV traveling westward from the Indian Monsoon until they dissipated over mainland Africa and observed the sea-level pressure at the same location. Identical circles are drawn on both the PV and SLP Hovmöller diagrams to visualize the same locations across diagrams (Figures 2 and 3).

We also provide an example of a PV map (Figure 4) to spatially show what the PV swaths from the Indian monsoon look like. We use these to visually confirm the patterns we observe in the Hovmöller diagrams.

Upon making the Hovmöller diagram for χ (Figure 5), a clear eastward movement was seen. Our area of interest being near the equator, we determined these to be the offshoots of equatorial Kelvin waves. Particularly strong waves then are associated with a divergence field (Nakamura and Takayabu 2022), which is seen on our Hovmöller diagram as a line of negative or near-zero χ. Lines are then drawn on Figure 5 to identify the movement of these disturbances.

Nine disturbances are identified, which would indicate the 2017 season to be a particularly active one given the reference of five-six Kelvin waves per year (Mekonnen et al. 2008).

As previously mentioned, we were also interested in how disturbances associated with AEWs are altered in the presence of Kelvin waves. To investigate this topic, we looked for evidence of the strongest disturbances of the 2017 hurricane season being connected with nearby Kelvin waves. When looking at the sea-level pressure Hovmöller diagram (Figure 6), a wall of red, high SLPs can be seen from the West African coast through the Caribbean, with some anomalously low SLP disturbances popping up in the Atlantic between 50W and 60W longitude. We drew circles around the lowest SLP disturbances in the Atlantic, with the later three of the four being Hurricanes Harvey, Irma, and Maria, respectively (Figure 6). We then overlayed these circles and the lines of Kelvin Waves from Figure 5 on top of the PV Hovmöller diagram (Figure 7) to investigate connections between AEWs and Kelvin waves.

There were multiple tradeoffs when deciding on an appropriate method for producing the Hovmöller diagrams. As previously mentioned, we aggregated the minimum values across the given latitude range because we were particularly interested in identifying swaths of low PV and divergence in the velocity potential field. This limited the acceptable latitude range for our analysis. We would have liked to extend the region of interest south to include all of India, to capture more of the Monsoon, and more of equatorial Africa, because there is evidence for two separate wave tracks of AEWs. One of these is at fifteen degrees north and the other at five degrees north (Diedhiou et al. 1999). Extending our analysis to five degrees north would have been problematic because plumes of low PV regularly extend northward from the equator, delivering energy and low PV to the midlatitudes. Examples of these plumes are circled in Figure 4 and more can be learned about them in Nyes and Tripoli (2019). The plumes of equatorial PV would show up as the minimum PV values in the Hovmöller diagrams far too often if we were to extend the region of interest southward.

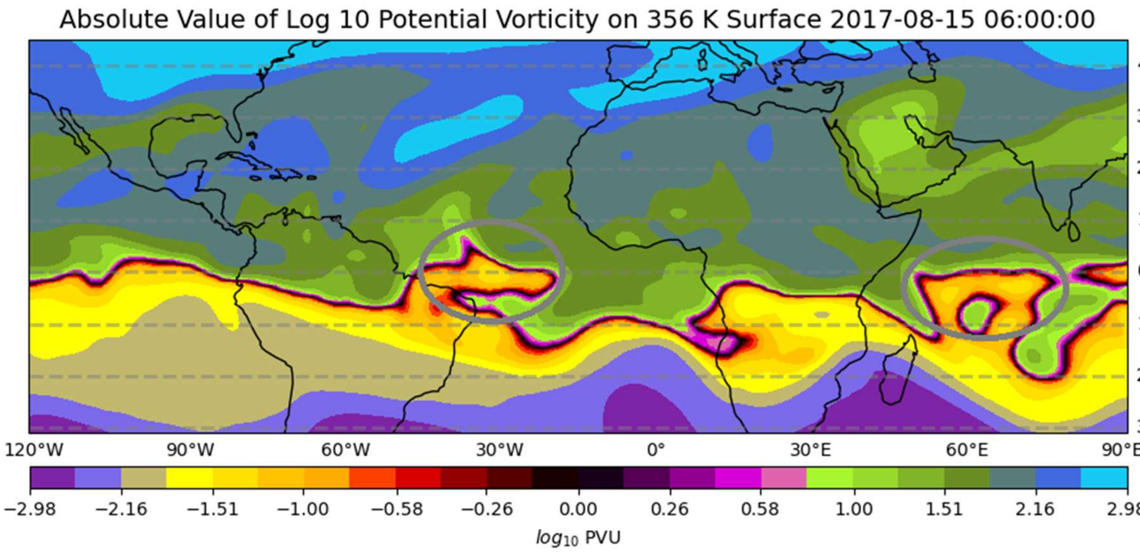

Figure 4: Map of potential vorticity data used for the Hovmöller diagrams in Figures 1, 2, and 7. Maps like this one were used to visually confirm the patterns seen in the Hovmöller diagrams. A plume of low PV air can be seen flowing from India into Saudi Arabia. Plumes of low equatorial PV are circled to demonstrate how extending the region of interest for Hovmöller diagrams would provide faulty results. This is because these plumes would be responsible for PV minimums instead of PV from the Indian Monsoon.

5. Data

The data used in this study is taken from the ECMWF ERA-Interim reanalysis dataset (Dee et al. 2011) and interpolated to the UW Nonhydrostatic Modeling System (UWNMS) grid (Tripoli and Smith 2014) to calculate dry variables. Data is chosen from the 2017 hurricane season due to the number of particularly strong hurricanes that year. The data has a (1^{o} latitude x 1^{o} longitude x 600 vertical m) grid spacing with heights starting at 300 m and going up to 34500 m. The data is taken between June 7 and October 31, 2017, and is indexed every 6 hours.

Potential vorticity data is taken on a log (base 10) scale to emphasize the near-zero values we were interested in for this study. Negative values have their absolute value taken for purposes of calculating their log but are returned to negative values afterwards.

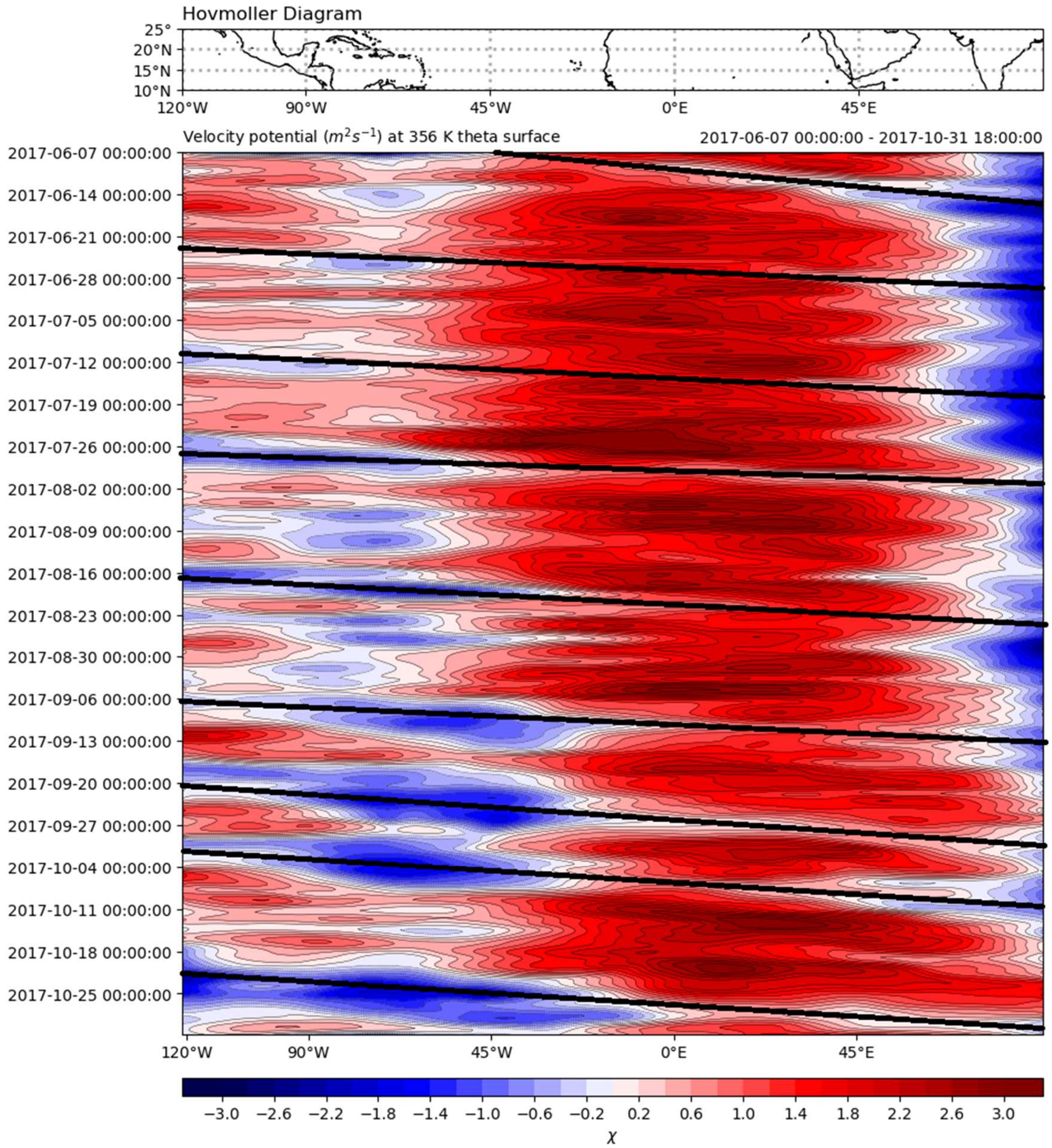

Figure 5: Hovmöller diagram of velocity potential (χ) with –χ showing divergence and +χ showing convergence. Colored values show the minimum χ value across all the latitudes in the defined range at a given time. Black lines show the approximate propagation of equatorial Kelvin waves carrying divergence fields. Identically positioned lines are drawn on Figure 7.

6. Results

As described in section 4, the first question we wanted to answer was whether there is an observable connection between swaths of low PV coming from the SAM at upper levels and a deepening of AEWs over Africa. Circles marking where PV anomalies that originate from the Indian Monsoon dissipate over mainland Africa are drawn on the PV Hovmöller diagram (Figure

2) and identical circles are drawn on the SLP Hovmöller diagram to investigate this question (Figure 3).

The results from this visualization are promising. In all cases except two, namely August 7 and August 15, the circles on Figure 3 line up closely with a localized SLP minimum. This relationship suggests that, upon PV plumes from the Indian Monsoon being deposited over Eastern Africa, an AEW is likely to deepen. It should be of note, however, that these lines were drawn by hand and there is nothing inherently numerical about them. A more numerical way of diagnosing this relationship should prove fruitful in the future.

We also wanted to diagnose whether the Kelvin waves we were observing in the χ field (Figure 5) had an observable effect on the strength of the AEWs. The strongest storms of the year, including Hurricanes Harvey, Irma, and Maria, are selected based off their low SLP signals in the Western Atlantic (Figure 6) to assess this relationship. The markings of Kelvin wave propagation and SLP minimums from Figures 5 and 6 are overlaid on the PV field from Figure 1 to get a full picture of this process (Figure 7). In each of the four storms marked in grey circles, we observe the presence of a Kelvin wave nearly right on top of the marker. From this, it appears that divergence fields being transported by equatorial Kelvin waves provide beneficial conditions for AEW-related disturbances to re-intensify in the Western Atlantic.

It is also interesting that, due to the apparent periodicity of Kelvin wave propagation, if you follow the orange lines of PV anomaly propagation in Figure 7 from each of the circled disturbances, a prior Kelvin wave was in the vicinity of the initial intensification of each of these storms in Eastern Africa, which we have associated with PV plumes. From this, it seems possible that some of the strongest storms in the Atlantic each year may be in sync with equatorial Kelvin wave propagation so that divergence fields aloft allow them to intensify both in Eastern Africa and in the Western Atlantic.

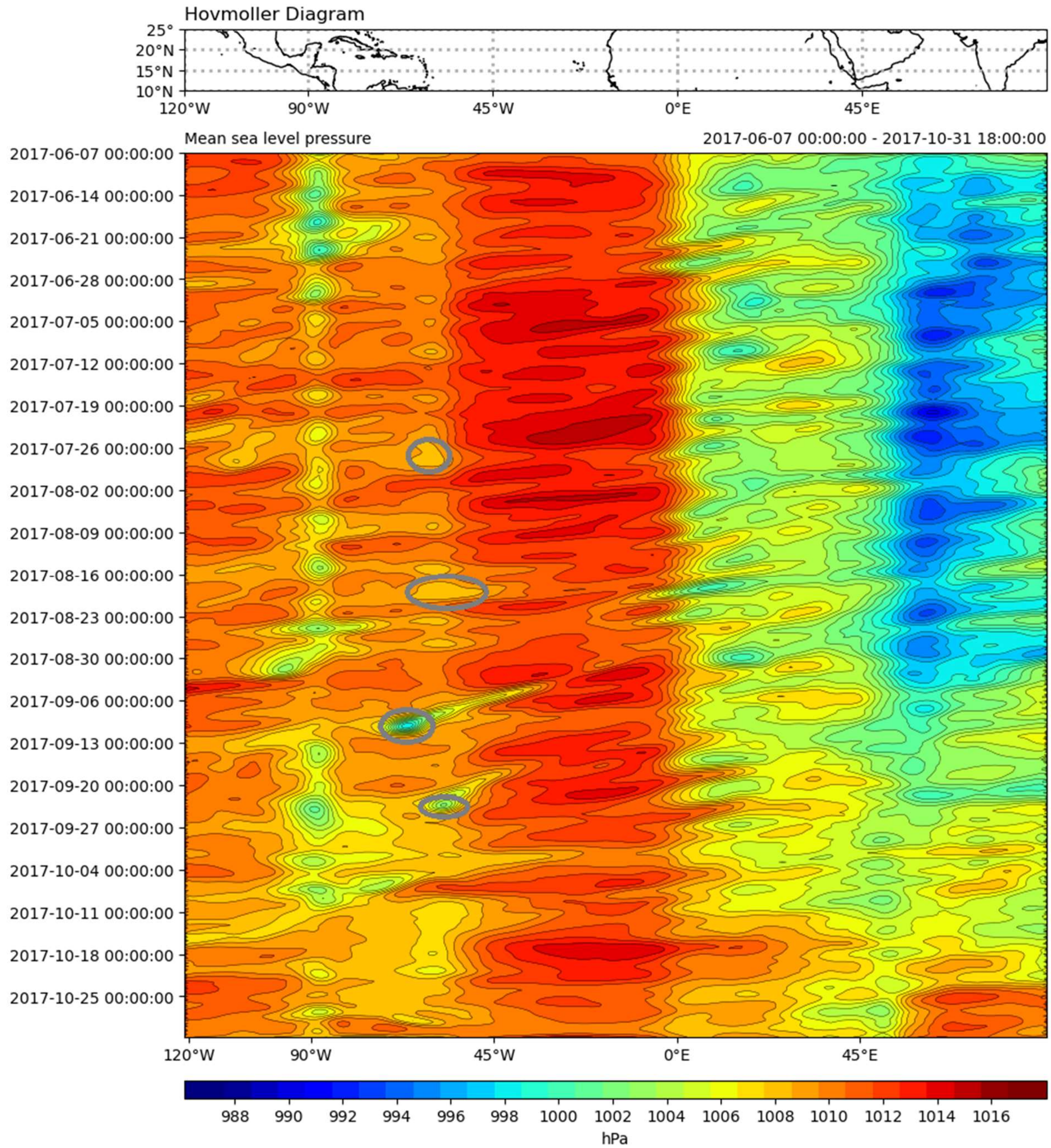

Figure 6: Same Hovmöller diagram as Figure 3 but with circles denoting specific low-pressure systems in the Western Atlantic. The bottom three circles denote Hurricanes Harvey, Irma, and Maria, respectively. Similarly positioned circles are drawn on Figure 7.

7. Future Work

As this is a primarily new viewpoint for AEW deepening, there are multiple areas for future work in the subject area. First would be a more quantitative analysis of the more qualitative trends shown in this study. A regression that relates upper air PV levels to the change in pressure over the same location which can give some sort of correlation value would provide a suitable mathematical model of the relationship we have described. This regression could be run at lag times of different hours to identify how quickly the influx of low PV is able to affect growing disturbances. One way to diagnose this relationship more in-depth would be to do a case study, potentially like Berry and Thorncroft (2005) did, but with a simulated idealized AEW. This would help provide a more controlled environment for analysis compared to our study, where AEWs throughout the 2017 season may have had significantly different structures.

As always, a simple way to further this research would be to use similar methods as we present in this study with different data and see whether the results agree with what we have found. We did some of the same analysis listed in this paper with data from the GFS model but ended up preferring ERA-I data due to its better spatial resolution. Other datasets could be explored to examine how strongly relationships proposed here show up.

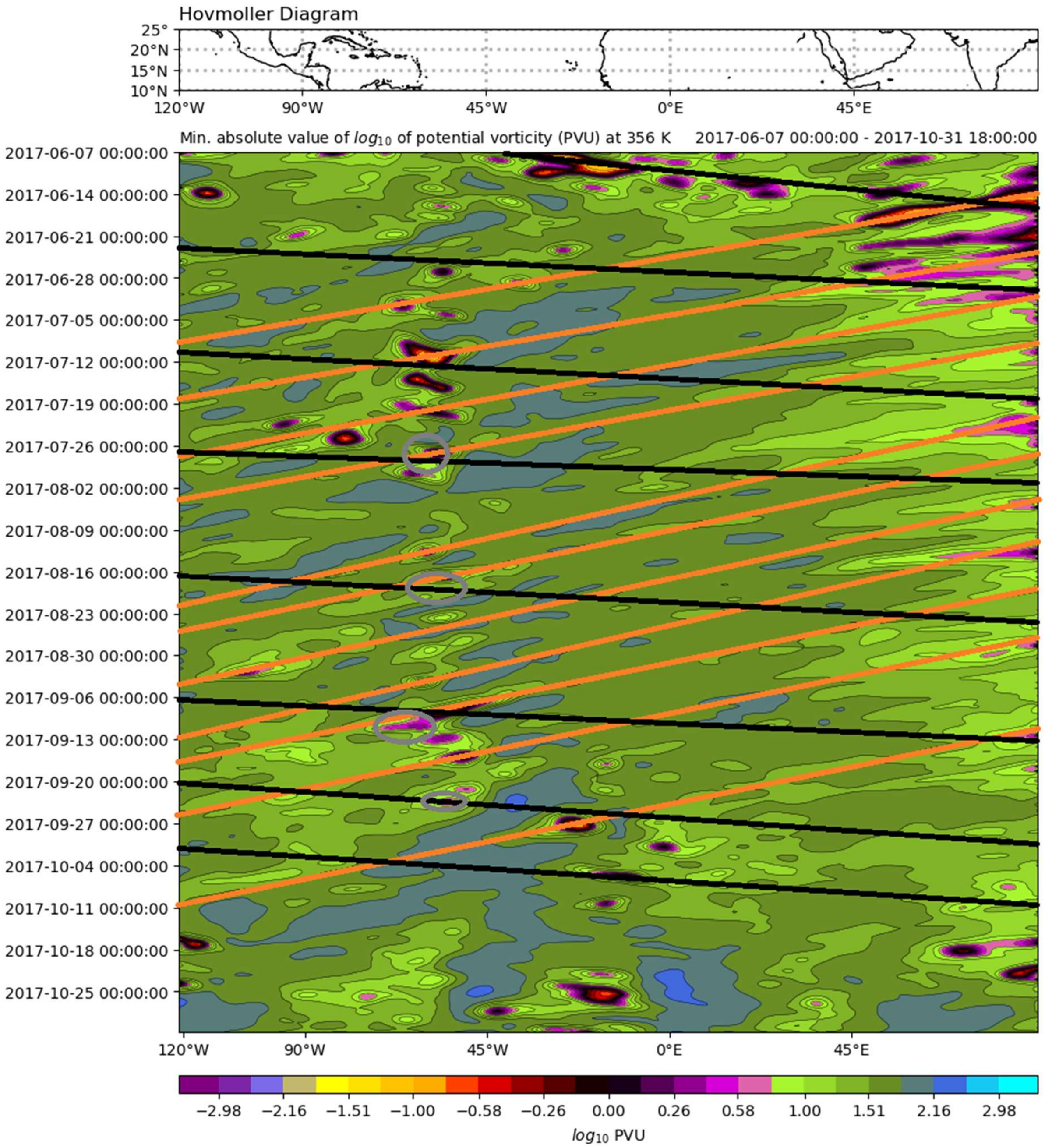

Figure 7: Same diagram as Figure 1 but with black lines from Figure 5 and grey circles from Figure 6 drawn on. Used to identify connections between deepening African Easterly Waves and Kelvin waves.

8. Summary and Conclusions

This study has tested the hypothesis that low PV air from the South Asian Monsoon provides environmental conditions beneficial for the upper tropospheric difluence observed to relate to the deepening of AEWs into intense hurricanes by Krishnamurti (2018) and that equatorial Kelvin waves bring divergence fields to further their deep convection. The use of multiple different Hovmöller diagrams was employed to track the movement of potential vorticity, velocity potential, and sea-level pressure anomalies between India and the Western Atlantic Ocean to investigate these relationships.

Good agreement was found between plumes of potential vorticity flowing from the Indian Monsoon and the initial intensification of AEWs over Northern Africa. This result backs up our hypothesis that these westward moving potential vorticity plumes are creating conditions that allow AEWs to deepen into intense disturbances. Moreover, there is evidence that the maturation of the SAM, during mid and late summer may account for the change in character of the AEWs moving off Africa from mid-July to September. Evidence was also proposed that shows that the most intense Atlantic storms of 2017, namely Harvey, Irma, and Maria, were able to intensify in the Western Atlantic partially due to divergence fields brought about by equatorial Kelvin waves. There is also evidence that the same intense storms may have been further influenced to deepen over Northern Africa due to the presence of prior Kelvin waves intersecting with low PV plumes from the SAM.

References

Albignat, J. P., and R. J. Reed, 1980: The Origin of African Wave Disturbances during Phase III of GATE. *Mon. Wea. Rev.*, **108**, 1827–1839, https://doi.org/10.1175/1520-0493(1980)108<1827:TOOAWD>2.0.CO;2.

Berry, G. J., and C. Thorncroft, 2005: Case Study of an Intense African Easterly Wave. *Mon. Wea. Rev.*, **133**, 752–766, https://doi.org/10.1175/MWR2884.1.

Burpee, R. W., 1972: The Origin and Structure of Easterly Waves in the Lower Troposphere of North Africa. *J. Atmos. Sci.*, **29**, 77–90, https://doi.org/10.1175/1520-0469(1972)029<0077:TOASOE>2.0.CO;2.

CARLSON, T. N., 1969: SOME REMARKS ON AFRICAN DISTURBANCES AND THEIR PROGRESS OVER THE TROPICAL ATLANTIC. *Mon. Wea. Rev.*, **97**, 716–726, https://doi.org/10.1175/1520-0493(1969)097<0716:SROADA>2.3.CO;2.

Dee et al., 2011, The ERA-Interim reanalysis: configuration and performance of the data assimilation system. *Q.J.R. Meteorol. Soc.*, **137**, 553-597. https://doi.org/10.1002/qj.828

Delden, A.V., 2003: Adjustment to heating, potential vorticity and cyclogenesis. *Q.J.R. Meteorol. Soc.*, **129**, 3305-3322. https://doi.org/10.1256/qj.01.65

Diedhiou, A., S. Janicot, A. Viltard, P. de Felice, and H. Laurent, 1999: Easterly wave regimes and associated convection over West Africa and tropical Atlantic: results from the NCEP/NCAR and ECMWF reanalyses. *Climate Dynamics,* **15**, 795–822, https://doi.org/10.1007/s003820050316.

Duvel, J. P., 1990: Convection over Tropical Africa and the Atlantic Ocean during Northern Summer. Part II: Modulation by Easterly Waves. *Mon. Wea. Rev.*, **118**, 1855–1868, https://doi.org/10.1175/1520-0493(1990)118<1855:COTAAT>2.0.CO;2.

Krishnamurti, T.N., N. Karmakar, V. Misra, B. Nag, D. Sahu, S. Dubey, and Z. Haddad, 2018: Association between upper level diffluence in the Tropical Easterly Jet and the formation of the strongest Atlantic hurricanes in recent years. *Proceedings of SPIE*, **10782**, https://doi.org/10.1117/12.2500287

Landsea, C. W., G. D. Bell, W. M. Gray, and S. B. Goldenberg, 1998: The Extremely Active 1995 Atlantic Hurricane Season: Environmental Conditions and Verification of Seasonal Forecasts. *Mon. Wea. Rev.*, **126**, 1174–1193, https://doi.org/10.1175/1520-0493(1998)126<1174:TEAAHS>2.0.CO;2.

Matthews, A. J., 2021: Dynamical propagation and growth mechanisms for convectively coupled equatorial Kelvin waves over the Indian Ocean. *Quarterly Journal of the Royal Meteorological Society*, *147*(741), 4310-4336, https://doi.org/10.1002/qj.4179.

Mekonnen, A., C. D. Thorncroft, A. R. Aiyyer, and G. N. Kiladis, 2008: Convectively Coupled Kelvin Waves over Tropical Africa during the Boreal Summer: Structure and Variability. *J. Climate*, **21**, 6649–6667, https://doi.org/10.1175/2008JCLI2008.1.

Nakamura, Y., and Y. N. Takayabu, 2022: Convective Couplings with Equatorial Rossby Waves and Equatorial Kelvin Waves. Part II: Coupled Precipitation Characteristics. *J. Atmos. Sci.*, **79**, 2919–2933, https://doi.org/10.1175/JAS-D-22-0003.1.

Nytes, L. E., and G. J. Tripoli, 2019: Seasonal and Subseasonal Variability of Potential Energy Injected into the Tropical UTLS by Convective and Tropical Cyclone Outflow. *J. Climate*, **32**, 8003–8017, https://doi.org/10.1175/JCLI-D-18-0303.1.

Persson, A., 2017: The Story of the Hovmöller Diagram: An (Almost) Eyewitness Account. *Bull. Amer. Meteor. Soc.*, **98**, 949–957, https://doi.org/10.1175/BAMS-D-15-00234.1.

Pytharoulis, I., and C. Thorncroft, 1999: The Low-Level Structure of African Easterly Waves in 1995. *Mon. Wea. Rev.*, **127**, 2266–2280, https://doi.org/10.1175/1520-0493(1999)127<2266:TLLSOA>2.0.CO;2.

Reed, R. J., and E. E. Recker, 1971: Structure and Properties of Synoptic-Scale Wave Disturbances in the Equatorial Western Pacific. *J. Atmos. Sci.*, **28**, 1117–1133, https://doi.org/10.1175/1520-0469(1971)028<1117:SAPOSS>2.0.CO;2.

Reed, R. J., D. C. Norquist, and E. E. Recker, 1977: The Structure and Properties of African Wave Disturbances as Observed During Phase III of GATE. *Mon. Wea. Rev.*, **105**, 317–333, https://doi.org/10.1175/1520-0493(1977)105<0317:TSAPOA>2.0.CO;2.

Schubert, W. H., and B. T. Alworth, 1987: Evolution of potential vorticity in tropical cyclones. *Q.J.R. Met. Soc.*, **113**, 147-162, https://doi.org/10.1002/qj.49711347509.

Takayabu, Y.N. (1994) Large-scale cloud disturbances associated with equatorial waves. Part I: spectral features of the cloud disturbances. *Journal of the Meteorological Society of Japan*, **72**, 433–448. https://doi.org/10.2151/jmsj1965.72.3_433.

Thorncroft, C., and K. Hodges, 2001: African Easterly Wave Variability and Its Relationship to Atlantic Tropical Cyclone Activity. *J. Climate*, **14**, 1166–1179, https://doi.org/10.1175/1520-0442(2001)014<1166:AEWVAI>2.0.CO;2.

Tripoli, G.J., and E. A. Smith, 2014: Introducing Variable-Step Topography (VST) coordinates within dynamically constrained Nonhydrostatic Modeling System (NMS). Part 1: VST formulation within NMS host model framework. *Dynamics of Atmospheres and Oceans*, **66**, 28-57, https://doi.org/10.1016/j.dynatmoce.2014.01.001.